





Remyelination of chronic demyelinated lesions with directly induced neural stem cells

Luca Peruzzotti-Jametti,¹ Nunzio Vicario,^{1,2} Giulio Volpe,¹ Sandra Rizzi,³ Cheek Kwok,⁴ Ivan Lombardi,^{1,5} Mads S. Bergholt,^{6,7} Lucas Barea-Moya,^{8,9,10} Andrea D'Angelo,¹ Alexandra M. Nicaise,¹ Giuseppe D'Amico,¹ Grzegorz Krzak,¹ Cory M. Willis,¹  Sara Gil-Perotin,^{8,9,11} Olena Hrubá,¹ Alice Braga,¹ Molly M. Stevens,⁷ José M. Garcia-Verdugo,⁸  Kourosh Saeb-Parsy,¹² Chao Zhao,¹³ Robin J. M. Franklin,¹³ Frank Edenhofer^{3,4} and Stefano Pluchino¹

The limited ability of CNS progenitor cells to differentiate into oligodendrocytes limits the repair of demyelinating lesions and contributes to the disability of people with progressive multiple sclerosis (PMS). Neural stem cell (NSC) transplantation has emerged as a safe therapeutic approach in people with PMS, where it holds the promise of healing the injured CNS. However, the mechanisms by which NSC grafts could promote CNS remyelination need to be carefully assessed before their widespread clinical adoption.

In this study, we used directly induced NSCs (iNSCs) as a novel transplantation source to boost remyelination in the CNS. Using a mouse model of focal lysophosphatidylcholine (LPC)-induced demyelination, we found that mouse iNSCs promote remyelination by enhancing endogenous oligodendrocyte progenitor cells differentiation and by directly differentiating into mature oligodendrocytes. Transplantation of mouse iNSCs in LPC-lesioned *Olig1*^{-/-} mice, which exhibits impaired remyelination, confirmed the direct remyelinating ability of grafts and the formation of new exogenous myelin sheaths. We also demonstrated that the xenotransplantation of human iNSCs (hiNSCs) is safe in mice, with hiNSCs persisting long-term in demyelinating lesions where they can produce graft-derived human myelin.

Our findings support the use of NSC therapies to enhance remyelination in chronic demyelinating disorders, such as PMS.

1 Department of Clinical Neurosciences and NIHR Biomedical Research Centre, University of Cambridge, Cambridge CB2 0AH, UK

2 Department of Biomedical and Biotechnological Sciences, Physiology Section, University of Catania, Catania I-95123, Italy

3 Institute of Molecular Biology & CMBI, Genomics, Stem Cell Biology & Regenerative Medicine, Leopold-Franzens-University Innsbruck, Innsbruck 6020, Austria

4 Institute of Anatomy and Cell Biology, University of Würzburg, Würzburg 97070, Germany

5 Department of Biotechnology and Biosciences, University of Milano-Bicocca, Milano 20126, Italy

6 Centre for Craniofacial & Regenerative Biology, King's College London, London WC2R 2LS, UK

7 Department of Materials, Department of Bioengineering, Institute of Biomedical Engineering, Imperial College London, London SW7 2AZ, UK

8 Laboratory of Comparative Neurobiology, Cavanilles Institute of Biodiversity and Evolutionary Biology, University of Valencia and CIBERNED-ISCIII, Valencia 46980, Spain

9 Research Group in Immunotherapy and Biomodels of Autoimmunity, Health Research Institute La Fe, Valencia 46026, Spain

Received November 15, 2024. Revised March 27, 2025. Accepted May 06, 2025. Advance access publication July 7, 2025

© The Author(s) 2025. Published by Oxford University Press on behalf of the Guarantors of Brain.

This is an Open Access article distributed under the terms of the Creative Commons Attribution License (<https://creativecommons.org/licenses/by/4.0/>), which permits unrestricted reuse, distribution, and reproduction in any medium, provided the original work is properly cited.

10 Department of Neurology, Hospital Universitario y Politécnico La Fe, Valencia 46026, Spain

11 Red Española de Terapias Avanzadas, TERA-V-RICORS, RD24/0014/0009, Instituto de Salud Carlos III, Sevilla 41092, Spain

12 Department of Surgery, Cambridge Biomedical Research Centre, University of Cambridge, Cambridge CB2 0QQ, UK

13 Wellcome Trust-Medical Research Council Cambridge Stem Cell Institute, Jeffrey Cheah Biomedical Centre, University of Cambridge, Cambridge CB2 0AW, UK

Correspondence to: Stefano Pluchino
 Department of Clinical Neurosciences
 University of Cambridge, Clifford Allbutt Building
 Hills Road, Cambridge CB2 0AH, UK
 E-mail: spp24@cam.ac.uk

Correspondence may also be addressed to: Luca Peruzzotti-Jametti
 E-mail: lp429@cam.ac.uk

Keywords: iNSC grafts; remyelination; multiple sclerosis; oligodendrocyte progenitor cells; demyelination; transplantation

Introduction

Multiple sclerosis (MS) is an immune mediated demyelinating disorder of the CNS and the most common cause of neurological disability in young adults.¹ Demyelination in MS is the result of complex interactions between the immune system and the CNS, which evolve over the disease course and a patient's lifetime.² In the early phase of MS, when infiltrating lymphocytes cause most of the CNS damage, the endogenous pool of oligodendrocyte progenitor cells (OPCs) can partially remyelinate demyelinating lesions by differentiating into mature, myelin-forming, oligodendrocytes (OLs). However, in the later chronic progressive stage of disease, this endogenous remyelination ability is severely insufficient.³ This leads to inadequate tissue repair and increasing lesion load, leading to the accumulation of disability seen in people with progressive multiple sclerosis (PMS).

Recent phase I clinical trials have demonstrated the safety and feasibility of neural stem cell (NSC) transplantation in people with PMS,^{4,5} paving the way for further research investigating its full therapeutic potential. Previous data obtained in preclinical models of MS-like diseases have shown that transplanted NSCs can significantly ameliorate clinico-pathological deficits of disease by exerting beneficial immunomodulatory and neurotrophic effects on the CNS.^{6,7} However, NSC grafts have shown a limited ability to replace damaged OLs and to generate new myelin *in vitro*, or when transplanted into highly inflammatory micro-environments.⁸ Stably expandable directly induced NSCs (iNSCs) from patients' skin fibroblasts offer an alternative source of NSCs for transplantation in people with PMS.^{8–10} This approach provides a rapid and scalable method for generating NSCs that circumvents ethical concerns and the need for immunosuppression.⁷ However, the effectiveness of these grafts to promote endogenous remyelination and/or directly producing new exogenous myelin remains unclear.

Our study aims to explore the potential of NSC grafts in promoting the remyelination of demyelinating lesions upon local intraparenchymal transplantation in the spinal cord. Through a comprehensive assessment of the differentiation ability of mouse NCS, mouse iNSCs and human iNSCs, we provide new evidence supporting the use of CNS specific transplantation therapies in chronic demyelinating disorders, such as PMS.

Materials and methods

Cell lines and *in vitro* culture

Details of all cell lines, their origin, and *n* per treatment group are reported in [Supplementary Table 1](#). Prior to all transplantation studies, cell viability was evaluated with trypan blue exclusion (>91% in all cell lines) and mycoplasma negative cells at passage $n \leq 30$ were used in all experiments. Further details are available in the [Supplementary material](#), 'Methods' section (including the lentiviral fGFP tagging).

Animals, focal demyelination of the spinal cord and cell transplantation

Spinal cord demyelinating lesions were induced in 8/12-week-old wild-type (WT) C57BL/6 or *Olig1*^{-/-} mice by stereotaxic injection of 1 μ l of 1% lysophosphatidylcholine (LPC, L4129 Sigma-Aldrich) between the T12 and T13 vertebrae (using a Hamilton syringe) reaching the ventral spinal cord, as previously described.¹¹ At 3 days post lesion (dpl), mice were randomized to receive either 1×10^5 cells in 1 μ l of PBS or an equal volume of the vehicle solution for PBS-treated mice. Further details of the methods [including *ex vivo* spinal cord histopathology, PCR, immunoblotting, *in situ* hybridization, transmission electron microscopy (TEM) and pre-embedding immunogold labelling, confocal Raman microspectroscopy, teratoma assay and statistical analyses] are available in the [Supplementary material](#), 'Methods' section.

Results

iNSC grafts integrate into the demyelinated spinal cord

To model CNS demyelination, we induced a focal lesion in the ventrolateral white matter of the spinal cord of C57BL/6 wild-type mice via a local LPC injection.¹¹ At 3 dpl, mice received an intralaminar injection of either mouse syngeneic fGFP⁺ iNSCs (iNSCs-treated), fGFP⁺ NSCs (NSCs-treated) or the vehicle solution (PBS-treated). Tissues were then collected at 10 and 21 dpl for downstream analyses ([Fig. 1A](#)).

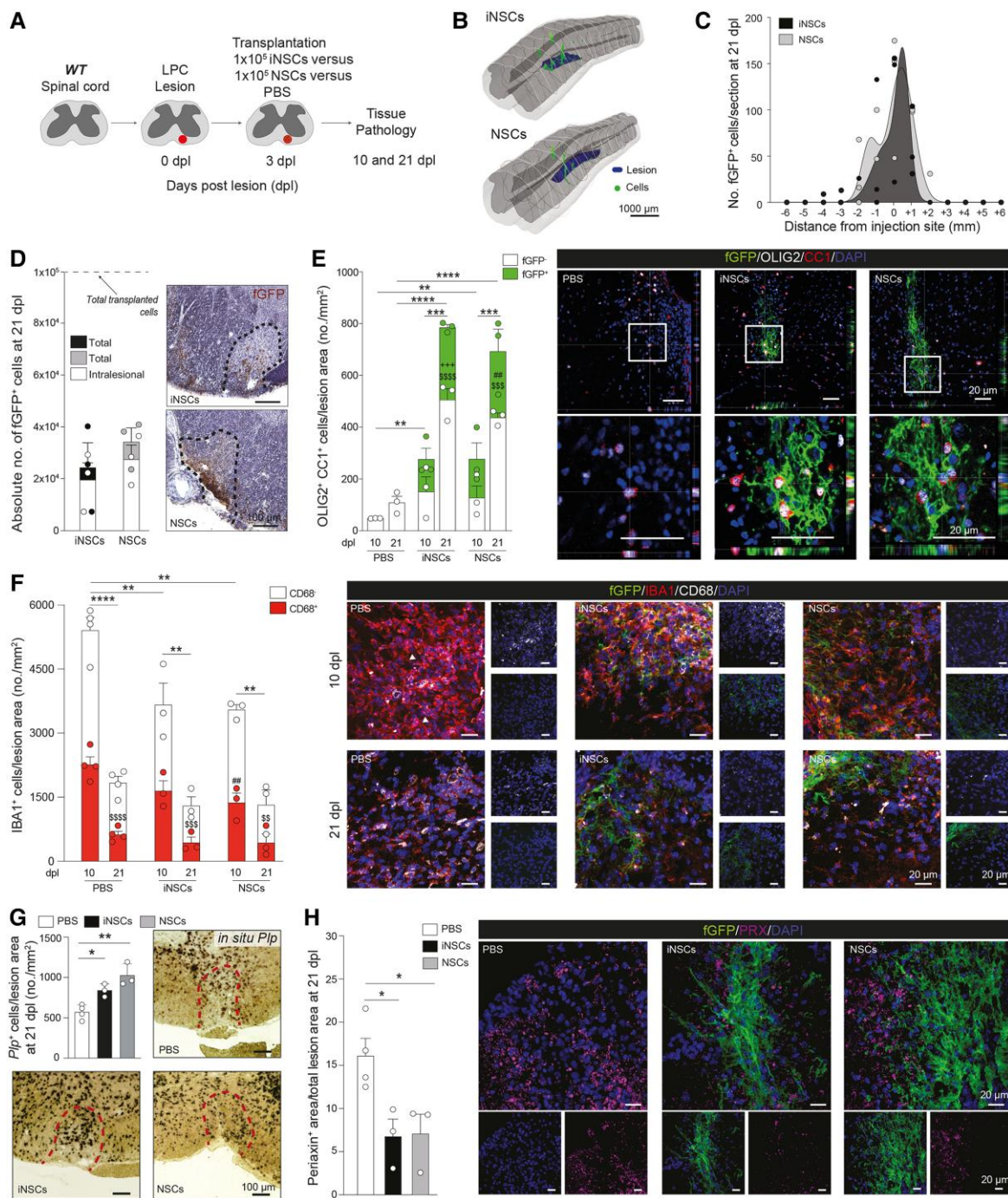


Figure 1 Transplanted mouse NSCs and induced NSCs survive, integrate and differentiate into fully mature oligodendrocytes in LPC spinal cord lesions of wild-type C57BL/6 mice. (A) Experimental setup for LPC-induced lesions and transplantation of mouse NSCs and iNSCs in wild-type (WT) C57BL/6 mice. (B) Representative 3D reconstructions showing individual transplanted fGFP⁺ cells (green shaded areas) in relation to the LPC-induced lesions of the ventral white matter of the spinal cord (blue shaded areas). (C and D) Stereology-based quantification of cell survival showing the distribution of fGFP⁺ iNSCs and fGFP⁺ NSCs (C) and absolute numbers of cells (total number and intralesional) with representative images (D). Data are mean values ± SEM analysed in *n* = 3 mice/group. (E) Quantification and representative images of endogenous (fGFP⁻) and exogenous (fGFP⁺) OLIG2⁺/CC1⁺ mature oligodendrocytes found in LPC-induced lesions of PBS-, iNSC- and NSC-treated mice. Data are mean values ± SEM analysed in *n* = 3 mice/group/time point. ***P* ≤ 0.01, ****P* ≤ 0.001, *****P* ≤ 0.0001; \$\$\$*P* ≤ 0.001, \$\$\$\$*P* ≤ 0.0001 versus PBS at 21 dpl; ****P* ≤ 0.001 versus GFP⁻ iNSC at 10 dpl; ##*P* ≤ 0.01 versus GFP⁻ NSC at 10 dpl. Two-way ANOVA, Tukey's multiple comparisons test. (F) Quantification and representative images of IBA1⁺ myeloid response and relative CD68 expression found in LPC-induced lesions of PBS-, iNSC- and NSC-treated mice. Data are mean values ± SEM analysed in *n* = 3 and *n* = 3 mice, respectively. ***P* ≤ 0.01, *****P* ≤ 0.0001; \$\$\$*P* ≤ 0.05, \$\$\$\$*P* ≤ 0.001, \$\$\$\$*P* ≤ 0.0001 comparing IBA1⁺/CD68⁺ between 21 dpl versus 10 dpl in the same group; ##*P* ≤ 0.01 versus PBS IBA1⁺/CD68⁺ at 21 dpl. Two-way ANOVA, Tukey's multiple comparisons test. (G) Quantification and representative images of *in situ* hybridization for Plp from PBS-, iNSC- and NSC-treated mice. Data are mean values ± SEM analysed in *n* = 4, *n* = 3 and *n* = 3 mice, respectively. **P* ≤ 0.05, ***P* ≤ 0.01. One-way ANOVA, Holm-Šidák's multiple comparison test. (H) Quantification and representative images of PRX⁺ area of PBS-, iNSC- and NSC-treated mice showing stem cell contribution to remyelinating the LPC-induced spinal cord lesions. Data are mean area/total lesion area ± SEM analysed in *n* = 4, *n* = 3, *n* = 3 mice, respectively. **P* ≤ 0.05. One-way ANOVA, Holm-Šidák's multiple comparison test. dpl = days post lesion; iNSC = induced neural stem cell; LPC = lysophosphatidylcholine; NSC = neural stem cell; SEM = standard error of the mean.

At 21 dpl, both iNSCs and NSCs successfully integrated into the demyelinated spinal cord, with cell density progressively decreasing from the injection site (Fig. 1B and C). A total of $24.3\% \pm 9.5\%$ and $34.2\% \pm 5.4\%$ transplanted cells survived at 21 dpl in iNSCs-treated and in NSCs-treated mice, respectively, with similar percentages of iNSCs and NSCs found intrasessionally (Fig. 1D). At 21 dpl, most transplanted cells expressed SOX1 ($71.4\% \pm 4.8\%$ and $66.5\% \pm 4.5\%$), while only a minority ($1.3\% \pm 0.7\%$ and $0.5\% \pm 0.3\%$) expressed the proliferation marker KI67 (Supplementary Fig. 1A and B). Both cellular grafts expressed the glial marker GFAP ($18.6\% \pm 2.5\%$ and $23.3\% \pm 4.1\%$) and, to a lower extent, the neuronal marker TUJ1 ($8.9\% \pm 3.2\%$ and $7.7\% \pm 2.7\%$).

When investigating the expression of markers indicative of oligodendroglial differentiation, we found that at 21 dpl, the subset of iNSCs and NSCs expressing the OPC markers NG2⁺/OLIG2⁺ ($2.9\% \pm 0.3\%$ and $4.0\% \pm 0.6\%$) was significantly lower than those expressing the mature OL markers OLIG2⁺/CC1⁺ ($8.5\% \pm 1.3\%$ and $11.5\% \pm 1.8\%$), which was 2.0-fold higher compared to an earlier time point (10 dpl) (Supplementary Fig. 1C and D), suggesting an increased differentiation of the grafts into OLs over time.

iNSC grafts increase the number of endogenous OLs and promote faster resolution of inflammatory myeloid responses

We next assessed how stem cell transplantation affected the remyelinating response after LPC injury by analysing the number of endogenous (fGFP⁻) versus exogenous (fGFP⁺) OLIG2⁺/CC1⁺ mature OLs at 10 and 21 dpl, intrasessionally.

Both iNSCs-treated and NSCs-treated wild-type mice displayed an increase in endogenous fGFP⁻ mature OLs versus control PBS-treated mice at 21 dpl (Fig. 1E). This enhanced endogenous response was coupled with a direct intrasessional differentiation of the grafts into fGFP⁺/OLIG2⁺/CC1⁺ cells, which significantly increased the total number of OLs intrasessionally versus PBS-treated mice (5.8-fold at 10 dpl and 7.2- and 6.4-fold at 21 dpl).

Since early myeloid cell activation in the LPC lesion model is known to exert anti-regenerative effects and limit remyelination,¹² we next examined the effects of grafts on microglia/macrophage numbers and polarisation (Fig. 1F). At 10 dpl, both iNSCs-treated and NSCs-treated wild-type mice showed a significant 1.5-fold reduction of total IBA1⁺ cells and IBA1⁺/CD68⁺ cells (1.4-fold and 1.6-fold) versus PBS-treated mice. At 21 dpl, the number of total IBA1⁺ and IBA1⁺/CD68⁺ cells was significantly reduced versus 10 dpl in all treatment groups.

In situ hybridization showed that both grafts induced a significant increase in the expression of Plp⁺ cells at 21 dpl intrasessionally versus PBS-treated mice (Fig. 1G), consistently with the increased number of total OLIG2⁺/CC1⁺ OLs.

Since previous data have shown that remyelination after demyelination of the spinal cord depends on both OLs derived from CNS-resident OPCs and Schwann cells (SCs) that originate from OPCs or the peripheral nervous system (PNS),¹¹ we next assessed the involvement of stem cells after transplantation. Both iNSCs-treated and NSCs-treated mice showed a significant reduction of PRX⁺, a myelin protein specific to the PNS that is absent in CNS myelin,¹³ versus PBS-treated mice at 21 dpl (Fig. 1H).

Altogether these findings suggest that both iNSC and NSC grafts foster remyelination in the injured spinal cord by exerting early immunomodulatory effects and reducing the contribution of stem cells, thus promoting more advantageous CNS specific

remyelination¹⁴ through enhanced endogenous OPC differentiation and direct differentiation into mature OLs.

iNSC grafts promote OL maturation and resolution of myeloid responses in *Olig1*^{-/-} demyelinated spinal cord

After observing comparable features of iNSC and NSC grafts *in vivo*, we next sought to investigate the direct role of iNSCs in CNS remyelination by transplanting them in a mouse model that displays impaired endogenous OL differentiation after injury. To this aim, we used *Olig1*^{-/-} mice (Supplementary Fig. 2A and B), which have normal endogenous OPC recruitment, but severely impaired OL differentiation in response to CNS injury.^{15,16} To assess the impact of the grafts on the incomplete remyelination of these transgenic mice, we focused on 21 dpl, a time point when WT mice exhibit instead a complete remyelination (Fig. 2A).

We found that iNSCs successfully integrated in the lesioned spinal cord of *Olig1*^{-/-} mice, with cell density progressively decreasing from the injection site (Fig. 2B and C). A total of $15.0\% \pm 5.7\%$ of transplanted iNSCs survived in the lesioned spinal cord at 21 dpl, with $13.7\% \pm 5.4\%$ of cells found intrasessionally (Fig. 2D).

Quantification of cell markers revealed that most transplanted cells expressed SOX1 ($68.7\% \pm 2.0\%$), while only a minority of iNSCs were proliferating ($2.0\% \pm 0.8\%$) (Supplementary Fig. 2C). Further *in vivo* differentiation profiling showed that iNSCs were expressing GFAP ($12.6\% \pm 0.8\%$), TUJ1 ($3.2\% \pm 1.1\%$), NG2/OLIG2 ($1.2\% \pm 0.8\%$) and OLIG2/CC1 ($9.0\% \pm 1.9\%$), similar to our results from wild-type transplanted mice.

We further investigated how iNSC transplantation contributed to the remyelinating response by assessing the number of endogenous and exogenous OLIG2⁺/CC1⁺ mature OLs at 21 dpl (Fig. 2E). We found that endogenous fGFP⁻/OLIG2⁺/CC1⁺ OLs in both iNSC-treated mice and PBS-treated at 21 dpl were very low (23.3 ± 10.5 cells/mm² versus 7.2 ± 3.6 cells/mm²), as expected.^{15,16} On the contrary, we found that a total of 196.07 ± 34.78 iNSCs/mm² differentiated into fGFP⁺/OLIG2⁺/CC1⁺ OLs, leading to a significant 30.4-fold increase in the total number of mature OLs versus PBS-treated *Olig1*^{-/-} mice (219.4 ± 39.3 versus 7.2 ± 3.6 cells/mm²).

When assessing myeloid cell reaction, we found that iNSC grafts induced a 1.4-fold significant reduction of total IBA1⁺ (1909 ± 197.2 cells/mm²) versus PBS-treated *Olig1*^{-/-} mice (2679 ± 229.1 cells/mm²) (Fig. 2F). *In situ* hybridization showed that the number of Plp⁺ cells was significantly increased in iNSC-treated versus PBS-treated *Olig1*^{-/-} mice (85.4 ± 17.6 cells/mm² versus 17.4 ± 6.3 cells/mm²) (Fig. 2G), while we found a significant reduction of PRX in iNSC-treated versus PBS-treated *Olig1*^{-/-} mice ($12.06\% \pm 2.77\%$ versus $21.98\% \pm 2.14\%$) (Fig. 2H).

Hence, iNSC grafts show immunomodulatory effects in the chronically demyelinated spinal cord white matter of *Olig1*^{-/-} mice, where they reduce the contribution of stem cells, and directly differentiate into myelin forming cells.

iNSC grafts directly remyelinate the chronically demyelinated spinal cord of *Olig1*^{-/-} mice

To assess the extent of remyelination induced by iNSC grafts, we next conducted ultrastructural TEM analyses of the LPC-lesioned spinal cords of iNSC-treated *Olig1*^{-/-} mice, PBS-treated *Olig1*^{-/-} mice and PBS-treated wild-type controls at 21 dpl.

PBS-treated *Olig1*^{-/-} mice exhibited a sustained extensive demyelination of LPC lesions, in line with a severe delay of their

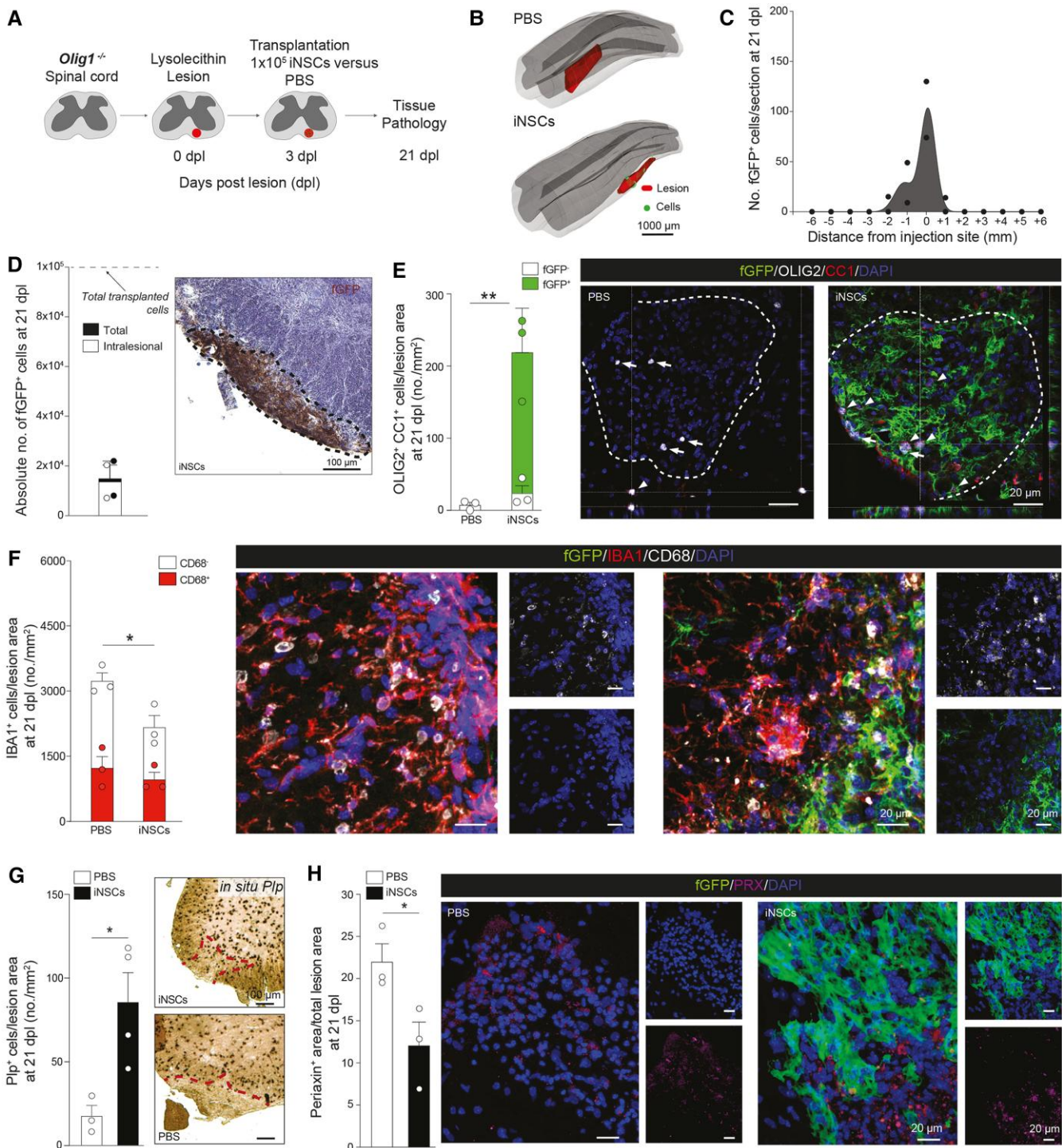


Figure 2 Transplanted mouse induced neural stem cells survive, integrate and generate mature oligodendrocytes in LPC spinal cord lesions of *Olig1*^{-/-} mice. (A) Experimental setup for LPC-induced lesions and transplantation of mouse iNSCs in *Olig1*^{-/-} mice. (B) Representative 3D reconstructions showing individual transplanted fGFP⁺ iNSCs (green shaded areas) in relation to the LPC-induced lesions of the ventral white matter of the spinal cord (red shaded areas). (C and D) Stereology-based quantification of cell survival showing the distribution of fGFP⁺ iNSCs (C) and absolute numbers of cells (total number and intralésional) with representative images (D). Data are mean values ± SEM analysed in *n* = 2 mice. (E) Quantification and representative images of endogenous (fGFP⁻) and exogenous (fGFP⁺) OLIG2⁺/CC1⁺ mature oligodendrocytes found in LPC-induced lesions of PBS- and iNSC-treated *Olig1*^{-/-} mice at 21 dpl. Data are mean values ± SEM analysed in *n* = 3 mice/group. ***P* ≤ 0.01. Unpaired t-test. (F) Quantification and representative images of IBA1⁺ myeloid response and relative CD68 expression found in LPC-induced lesions of PBS- and iNSC-treated *Olig1*^{-/-} mice at 21 dpl. Data are mean values ± SEM analysed in *n* = 3 mice/group. **P* ≤ 0.05. Unpaired t-test. (G) Quantification and representative images of *in situ* hybridization for Plp from PBS- and iNSC-treated *Olig1*^{-/-} mice at 21 dpl. Data are mean values ± SEM analysed in *n* = 3, *n* = 4 mice, respectively. **P* ≤ 0.05. Unpaired t-test. (H) Quantification and representative images of PRX⁺ area of PBS- and iNSC-treated *Olig1*^{-/-} mice showing stem cell contribution to remyelinating LPC-induced spinal cord lesions at 21 dpl. Data are mean area/total lesion area ± SEM analysed in *n* = 3 mice/group. **P* ≤ 0.05. Unpaired t-test. dpl = days post lesion; iNSC = induced neural stem cell; LPC = lysophosphatidylcholine; SEM = standard error of the mean.

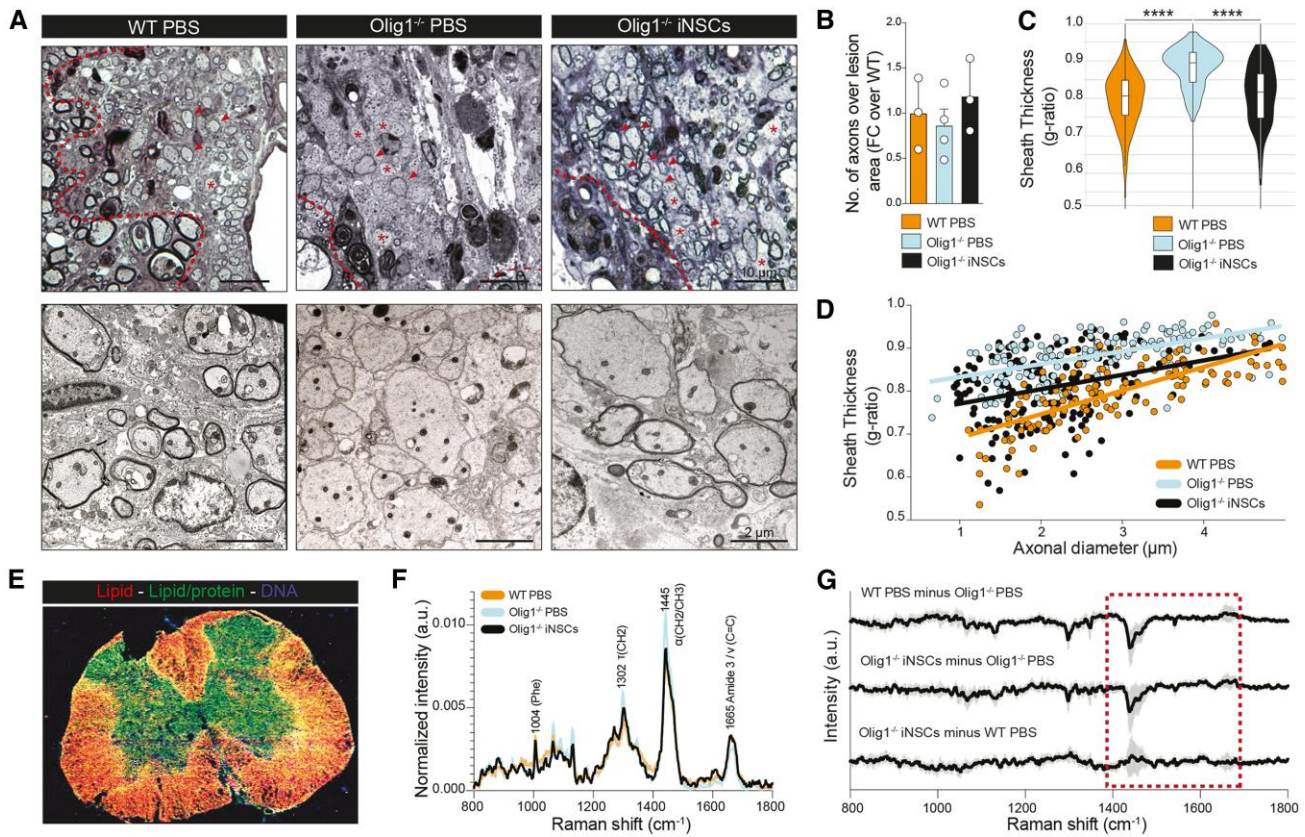


Figure 3 Transplanted mouse induced neural stem cells remyelinate LPC lesions of Olig1^{-/-} mice. (A) Representative pictures of toluidine blue stained LPC lesions (top) and corresponding TEM images (bottom) of PBS-treated wild-type (WT) mice, PBS-treated Olig1^{-/-} mice and iNSC-treated Olig1^{-/-} mice. Asterisks indicate demyelinated axons, arrowheads indicate remyelinated axons, dashed lines indicate the border of the lesion. (B) Quantification of the total number of axons per lesion area in PBS-treated WT mice (n = 3), PBS-treated Olig1^{-/-} mice (n = 4) and iNSC-treated Olig1^{-/-} mice (n = 3). (C and D) Quantification of the g-ratio of axons within the demyelinated lesion of PBS-treated WT mice, PBS-treated Olig1^{-/-} mice and iNSC-treated Olig1^{-/-} mice. Data are mean ± min max values (C) and single values plotted on axonal diameter (D). ****P ≤ 0.0001. One way ANOVA, Holm-Šidák's multiple comparisons test. (E) Confocal Raman imaging of a representative LPC lesion (from PBS-treated Olig1^{-/-} mouse) at 21 dpl, showing peaks associated with lipids (1445 cm⁻¹), lipid/protein (1665 cm⁻¹) and DNA (1345 cm⁻¹). (F) Mean Raman spectra of lesions in PBS-treated WT (n = 3), PBS-treated Olig1^{-/-} (n = 5) and iNSC-treated Olig1^{-/-} mice (n = 3) at 21 dpl. Peaks associated with myelin/lipids [1302 cm⁻¹ τ(CH2), 1445 cm⁻¹ α(CH2/CH3) and 1665 cm⁻¹ ν(C=C)] or axons/proteins [e.g. 1004 (phenylalanine)] are labelled. (G) Mean difference spectra (±1 standard deviation) of LPC lesions at 21 dpl, comparing the three different groups: PBS-treated WT (n = 3), PBS-treated Olig1^{-/-} (n = 5) and iNSC-treated Olig1^{-/-} (n = 3) mice. PBS-treated WT and iNSC-treated Olig1^{-/-} minus PBS-treated Olig1^{-/-} difference spectra (top two lines) show major differences, while PBS-treated WT and iNSC-treated Olig1^{-/-} difference spectra (bottom line) are superimposable. Red dotted box outlines peaks associated with myelin/lipids. dpl = days post lesion; iNSC = induced neural stem cell; LPC = lysophosphatidylcholine; min = minimum; max = maximum; TEM = transmission electron microscopy.

remyelination processes^{15,16} (Fig. 3A). Instead, iNSC-treated Olig1^{-/-} mice showed active remyelination of lesions, which was superimposable to the spontaneous remyelinating response seen in wild-type mice. While we did not detect striking features of axonal degeneration, nor significant changes in the number of axons among treatment groups (Fig. 3B), we found a significant decrease of axonal g-ratios in iNSC-treated Olig1^{-/-} mice (0.80 ± 0.006) versus PBS-treated Olig1^{-/-} mice (0.88 ± 0.004), almost reaching values observed in PBS-treated wild-type mice (0.79 ± 0.006 ; Fig. 3C and D).

We further analysed the molecular composition of LPC lesions at 21 dpl, using confocal Raman microspectroscopy (Fig. 3E), an approach that has high sensitivity to myelin [particularly around 1302 cm⁻¹ τ(CH2), 1445 cm⁻¹ α(CH2/CH3) and 1665 cm⁻¹ ν(C=C) of lipids].¹⁷ The mean Raman spectra showed no significant differences in protein related peaks [e.g. 1004 (phenylalanine) or 1227–1272 (Amide III)] associated with axons¹⁷ (Fig. 3F). We then analysed the mean difference spectra (±1 standard deviation) and found

instead that both PBS-treated wild-type and iNSC-treated Olig1^{-/-} mice displayed a very different molecular lesional profile versus PBS-treated Olig1^{-/-} mice, especially in Raman peaks associated with myelin (Fig. 3G). On the contrary, the lesional myelin composition of iNSC-treated Olig1^{-/-} mice closely resembled the spontaneous remyelination of PBS-treated wild-type mice (Fig. 3G), with higher myelin index versus PBS-treated Olig1^{-/-} mice (Supplementary Fig. 3).

Altogether, these data show that iNSCs have the potential to directly differentiate in OLs and drive myelin formation, even when transplanted in lesions where endogenous remyelinating processes are chronically impaired.

Human iNSC xenografts are safe and survive in chronically demyelinated spinal cord of Olig1^{-/-} mice

We next reprogrammed human iNSCs (hiNSCs) from dermal fibroblasts¹⁰ for xenotransplantation studies (Supplementary Fig. 4A).

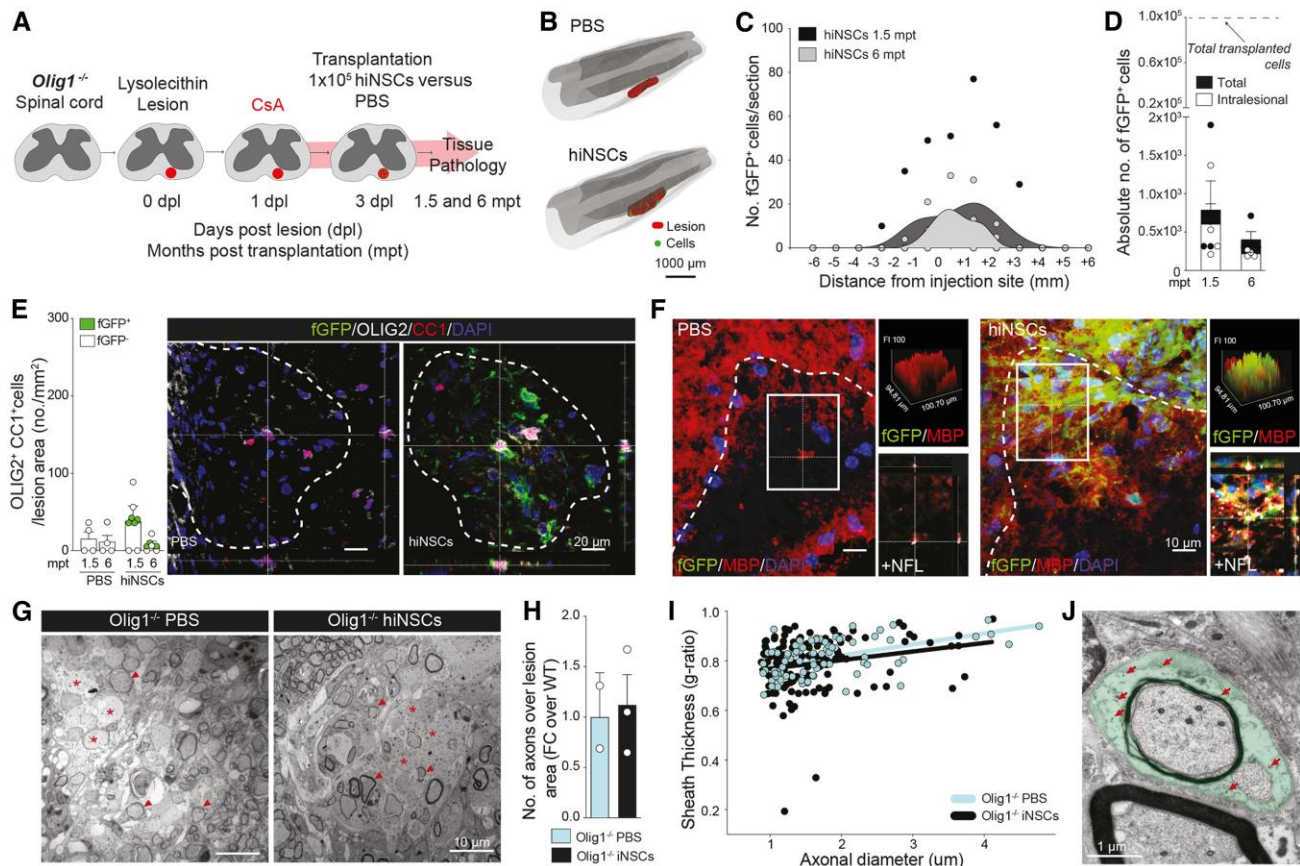


Figure 4 Transplanted human induced neural stem cells survive, integrate and differentiate in mature oligodendrocytes in LPC spinal cord lesions of *Olig1*^{-/-} mice. (A) Experimental setup for LPC-induced lesions and transplantation of hiNSCs in *Olig1*^{-/-} mice. (B) Representative 3D reconstructions showing individual transplanted fGFP⁺ hiNSCs (green shaded areas) in relation to the LPC-induced lesions of the ventral white matter of the spinal cord (red shaded areas). (C and D) Stereology-based quantification of cell survival showing distribution of fGFP⁺ hiNSCs (C) with absolute numbers of cells (total number and intralesional) (D). Data are mean values \pm SEM analysed in $n = 4$ mice at 1.5 mpt and $n = 4$ mice at 6 mpt. (E) Quantification and representative images of endogenous (fGFP⁺) and exogenous (fGFP⁺) OLIG2⁺/CC1⁺ mature oligodendrocytes found in LPC-induced lesions of PBS- and hiNSC-treated mice. Data are mean values \pm SEM analysed in $n = 4$ mouse/group/time point. (F) Representative images of immunofluorescence stainings for MBP (myelin marker) and fGFP⁺ within lesions (maximum projections are shown on the left). Right: Respective qualitative histograms of the lesions (top) and single z-stack of the inset shown in the maximum projection with added NFL staining for axons (bottom). (G) Representative TEM images of LPC lesions from PBS-treated *Olig1*^{-/-} and hiNSC-treated *Olig1*^{-/-} mice at 6 mpt. Asterisks indicate demyelinated axons, arrowheads indicate remyelinated axons. (H) Quantification of the total number of axons per lesion area in PBS-treated *Olig1*^{-/-} mice ($n = 2$) and hiNSC-treated *Olig1*^{-/-} mice ($n = 3$). (I) Quantification of the g-ratio of axons within the demyelinated lesion of PBS-treated *Olig1*^{-/-} mice ($n = 2$) and hiNSC-treated *Olig1*^{-/-} mice ($n = 3$). Data are single values plotted on axonal diameter. (J) Representative TEM image showing fGFP⁺ hiNSCs (pseudocoloured in green) wrapping around an axon within LPC lesions. Arrows show immunogold labelling for fGFP. hiNSC = human induced neural stem cell; LPC = lysophosphatidylcholine; mpt = months post transplantation; SEM = standard error of the mean; TEM = transmission electron microscopy; WT = wild-type.

Prior to transplantation, fGFP⁺ hiNSCs (Supplementary Fig. 4B) were negative for the pluripotency marker Oct4 (Supplementary Fig. 4C), while showing sustained expression of both SOX1 and SOX2 *in vitro* (Supplementary Fig. 4D).

We first transplanted fGFP⁺ hiNSCs, or control fGFP⁺ hiPSCs, under the kidney capsule of NOD SCID mice,¹⁸ to assess their tumorigenicity *in vivo*. While hiPSC-treated mice showed consistent teratoma formation at 70 dpt, no teratomas were ever seen in the hiNSC-treated group (Supplementary Fig. 5A–C). We next investigated hiNSC grafts survival and integration in the lesioned spinal cord of immunosuppressed *Olig1*^{-/-} mice (Fig. 4A).

We found that hiNSC grafts were able to persist in the spinal cord of all transplanted mice at 1.5- and 6-months post transplantation (mpt), with cell density progressively decreasing from the injection site (Fig. 4B and C). However, compared to mouse iNSCs, the survival rate of hiNSCs in the mouse spinal cord was relatively low

(0.8% \pm 0.4% and 0.4% \pm 0.1% of transplanted cells at 1.5 and 6 mpt, respectively) (Fig. 4D).

Nonetheless, we found that hiNSC xenografts were able differentiate into mature OLs intralesionally (2.8 ± 1.6 fGFP⁺/OLIG2⁺/CC1⁺ cells/mm² found in $n = 2/4$ mice at 1.5 mpt; and 1.1 fGFP⁺/OLIG2⁺/CC1⁺ cells/mm² found in $n = 1/4$ mice at 6 mpt) (Fig. 4E), where human fGFP⁺ MBP⁺ myelin was also observed (Fig. 4F).

Ultrastructurally, TEM analyses of hiNSC-treated *Olig1*^{-/-} mice and PBS-treated *Olig1*^{-/-} mice showed incomplete remyelination of LPC spinal cord lesions at 6 mpt, although few remyelinated axons that could be seen in both groups (Fig. 4G). While we did not observe significant axonal degeneration, nor significant changes in the number of axons within lesions (Fig. 4H), we found that the g-ratio was lower, albeit not significantly, in hiNSC-treated versus PBS-treated *Olig1*^{-/-} mice [0.79 ± 0.010 versus 0.81 ± 0.008 (standard error of the mean)] (Fig. 4I). These data were associated with the

finding of fgGFP⁺ hiNSCs wrapping around axons within *Olig1*^{-/-} lesions at 6 mpt (Fig. 4).

These results support the safety, and the potential for long-term integration, of hiNSCs *in vivo*, highlighting their potential therapeutic use in fostering remyelination of chronically demyelinated lesions.

Discussion

Stem cell transplantation is a promising approach for treating multifactorial neurological disorders.⁷ NSCs have unique benefits, such as immune modulation and trophic support, as well as the potential to replace damaged CNS cells.¹⁹ However, prior animal models of MS-like diseases demonstrated limited direct remyelination by NSC grafts, as most transplanted cells remained undifferentiated in atypical perivascular niches.^{6,8,20}

In this study, we used a focal demyelination model of the spinal cord to study how NSC transplantation affects remyelination after damage. We found that transplanted mouse NSCs and iNSCs stimulated the formation of endogenous mature OLs in wild-type mice as described,²¹ possibly through the secretion of growth factors like BDNF and IGF-1²² or by reducing inflammatory myeloid responses.¹² Importantly, we observed that some transplanted iNSCs also differentiated into astrocytes, which may play a crucial role in promoting CNS-dependent remyelination. This is consistent with evidence that astrocytes support the differentiation of OPCs into mature OLs while inhibiting SC-mediated remyelination.¹¹

In addition, we show that iNSC grafts can also directly differentiate into mature OLs within lesions of wild-type mice, potentially driven by SHH, BMPs or WNT intracellular signalling pathways.²³ However, since this process occurs in competition with the endogenous remyelination response,²⁴ we next used *Olig1*^{-/-} mice to abolish graft-host competition in the remyelination process. Using this model of significantly impaired (up to 6 months) endogenous remyelination, we were able to fully establish that transplanted iNSCs can indeed produce mature OLs that effectively remyelinate the CNS.

Using this transgenic model, our study also provides preliminary evidence supporting the remyelination capability of hiNSCs in chronically demyelinated lesions. These results complement previous studies in which other genetic (i.e. shiverer mice) or toxin-induced (i.e. cuprizone) animal models of hypo/demyelination were used to assess the oligodendroglial potential of human stem/precursor cell grafts.^{25,26} Future studies will need to investigate if hiNSCs harbour direct or indirect remyelination ability in wild-type mice and in more physiological models of delayed remyelination (e.g. aged mice).

Although we demonstrate that hiNSCs are safe for transplantation and have the potential of integrating and producing myelin in chronic demyelinated lesions, the use of iNSCs from healthy fibroblast lines limits our ability to study patient-specific traits that may impact their remyelinating efficacy.^{27,28} The limited number of cells retrieved is also a clear limitation, underscoring the need for future research on alternative transplantation doses and immunosuppression protocols. Since our intralésional transplantation approach may not be clinically feasible to treat multiple demyelinating lesions in human neurological disorders, future studies should also investigate alternative delivery methods, such as intrathecal or intracerebroventricular routes.

In conclusion, our findings support the effectiveness of iNSCs as a strategy with minimal immunogenicity and proven immunomodulatory abilities, offering strong evidence for enhanced

remyelination driven by the graft, paving the way for future therapeutic applications in regenerative neuroimmunology.

Data availability

Data supporting the findings of this study are available within the article and its [Supplementary material](#). Raw data are available from the corresponding authors upon request.

Acknowledgements

The authors thank P. Brophy (for kindly providing the anti-PRX antibody), B. Balzarotti, G. Gonzalez, D. Morrison, G. Pluchino, D. Trajkovski, and current/previous members of the Pluchino laboratory. The thumbnail image for the online table of contents was created in BioRender. Pluchino, S. (2025) <https://BioRender.com/aoir7t8>.

Funding

This work was supported by Wellcome Trust Research Training Fellowship (G105713, RG79423) and a National Multiple Sclerosis Society Grant (RFA-2203-39318) to L.P.J.; International PhD program in Neuroscience to N.V.; Italian Multiple Sclerosis Association (AISM/FISM) Cod. 2014/PMS/4 to G.V.; PhD Fellowship from the Italian Ministry of University and Research, and an Exchange EXTRA-EU Fellowship from the University of Milano-Bicocca to I.L.; 'Post-residency Grant' from the Health Research Institute La Fe and PI23/01037 from the Instituto de Salud Carlos III to L.B.M.; ECTRIMS Postdoctoral Research Fellowship Exchange Program (G104956) and UK Multiple Sclerosis Society Centre Excellence grant (G118541) to A.M.N.; National MS Society Post-doctoral fellowship (FG-2008-36954) to C.M.W.; 'Juan Rodes Grant' from the Instituto de Salud Carlos III (JR20/00033) and TERAV-RICOTS (RD24/0014/0009) and PI23/01037 from the Instituto de Salud Carlos III to S.G.P.; Valencian Council for Education, Culture, University and Employment (CIPROM/2023/053) and CIBER network (CB06/05/1131) to J.M.G.V. (and S.G.P.); UK Regenerative Medicine Platform grants 'Acellular Approaches for Therapeutic Delivery' (MR/K026682/1) and 'A Hub for Engineering and Exploiting the Stem Cell Niche' (MR/K026666/1) to M.M.S.; Dr Miriam and Sheldon G Adelson Medical Research Foundation and core support grant from the Wellcome Trust-MRC Cambridge Stem Cell Institute (203151/Z/16/Z) to R.J.M.F.; ERA-Net E-rare research programme and the Austrian Science Fund (FWF) to F.E.; and AISM/FISM, the Italian Ministry of Health, the ERC, the Medical Research Council, the Bascule Charitable Trust, and the Wellcome Trust-MRC Cambridge Stem Cell Institute to S.P.

Competing interests

S.P. is founder, CSO and shareholder (>5%) of CITC Ltd. The other authors report no competing interests.

Supplementary material

[Supplementary material](#) is available at *Brain* online.

References

1. Reich DS, Lucchinetti CF, Calabresi PA. Multiple sclerosis. *N Engl J Med*. 2018;378:169–180.

2. Graves JS, Krysko KM, Hua LH, Absinta M, Franklin RJM, Segal BM. Ageing and multiple sclerosis. *Lancet Neurol.* 2023;22:66-77.
3. Franklin RJM. Why does remyelination fail in multiple sclerosis? *Nat Rev Neurosci.* 2002;3:705-714.
4. Leone MA, Gelati M, Profico DC, et al. Phase I clinical trial of intracerebroventricular transplantation of allogeneic neural stem cells in people with progressive multiple sclerosis. *Cell Stem Cell.* 2023;30:1597-1609.e8.
5. Genchi A, Brambilla E, Sangalli F, et al. Neural stem cell transplantation in patients with progressive multiple sclerosis: An open-label, phase 1 study. *Nat Med.* 2023;29:75-85.
6. Pluchino S, Quattrini A, Brambilla E, et al. Injection of adult neurospheres induces recovery in a chronic model of multiple sclerosis. *Nature.* 2003;422:688-694.
7. Pluchino S, Smith JA, Peruzzotti-Jametti L. Promises and limitations of neural stem cell therapies for progressive multiple sclerosis. *Trends Mol Med.* 2020;26:898-912.
8. Peruzzotti-Jametti L, Bernstock JD, Vicario N, et al. Macrophage-derived extracellular succinate licenses neural stem cells to suppress chronic neuroinflammation. *Cell Stem Cell.* 2018;22:355-368.e13.
9. Thier M, Worsdorfer P, Lakes YB, et al. Direct conversion of fibroblasts into stably expandable neural stem cells. *Cell Stem Cell.* 2012;10:473-479.
10. Meyer S, Worsdorfer P, Gunther K, Thier M, Edenhofer F. Derivation of adult human fibroblasts and their direct conversion into expandable neural progenitor cells. *J Vis Exp.* 2015;101:e52831.
11. Zawadzka M, Rivers LE, Fancy SP, et al. CNS-resident glial progenitor/stem cells produce Schwann cells as well as oligodendrocytes during repair of CNS demyelination. *Cell Stem Cell.* 2010;6:578-590.
12. Lloyd AF, Davies CL, Holloway RK, et al. Central nervous system regeneration is driven by microglia necroptosis and repopulation. *Nat Neurosci.* 2019;22:1046-1052.
13. Gillespie CS, Sherman DL, Blair GE, Brophy PJ. Periaxin, a novel protein of myelinating Schwann cells with a possible role in axonal ensheathment. *Neuron.* 1994;12:497-508.
14. Chen CZ, Neumann B, Forster S, Franklin RJM. Schwann cell remyelination of the central nervous system: Why does it happen and what are the benefits? *Open Biol.* 2021;11:200352.
15. Arnett HA, Fancy SP, Alberta JA, et al. bHLH transcription factor Olig1 is required to repair demyelinated lesions in the CNS. *Science (New York, NY).* 2004;306:2111-2115.
16. Lu QR, Sun T, Zhu ZM, et al. Common developmental requirement for Olig function indicates a motor neuron/oligodendrocyte connection. *Cells.* 2002;109:75-86.
17. Bergholt MS, Serio A, McKenzie JS, et al. Correlated heterospectral lipidomics for biomolecular profiling of remyelination in multiple sclerosis. *ACS Cent Sci.* 2018;4:39-51.
18. Georgakopoulos N, Prior N, Angres B, et al. Long-term expansion, genomic stability and in vivo safety of adult human pancreas organoids. *BMC Dev Biol.* 2020;20:4.
19. Fischbach MA, Bluestone JA, Lim WA. Cell-based therapeutics: The next pillar of medicine. *Sci Transl Med.* 2013;5:179ps7.
20. Pluchino S, Muzio L, Imitola J, et al. Persistent inflammation alters the function of the endogenous brain stem cell compartment. *Brain.* 2008;131(Pt 10):2564-2578.
21. Sullivan GM, Knutsen AK, Peruzzotti-Jametti L, et al. Transplantation of induced neural stem cells (iNSCs) into chronically demyelinated corpus callosum ameliorates motor deficits. *Acta Neuropathol Commun.* 2020;8:84.
22. Willis CM, Nicaise AM, Peruzzotti-Jametti L, Pluchino S. The neural stem cell secretome and its role in brain repair. *Brain Research.* 2020;1729:146615.
23. Radecki DZ, Samanta J. Endogenous neural stem cell mediated oligodendrogenesis in the adult mammalian brain. *Cells.* 2022;11:2101.
24. Mozafari S, Laterza C, Roussel D, et al. Skin-derived neural precursors competitively generate functional myelin in adult demyelinated mice. *J Clin Invest.* 2015;125:3642-3656.
25. Uchida N, Chen K, Dohse M, et al. Human neural stem cells induce functional myelination in mice with severe dysmyelination. *Sci Transl Med.* 2012;4:155ra136.
26. Windrem MS, Schanz SJ, Guo M, et al. Neonatal chimerization with human glial progenitor cells can both remyelinate and rescue the otherwise lethally hypomyelinated shiverer mouse. *Cell Stem Cell.* 2008;2:553-565.
27. Ionescu RB, Nicaise AM, Reisz JA, et al. Increased cholesterol synthesis drives neurotoxicity in patient stem cell-derived model of multiple sclerosis. *Cell Stem Cell.* 2024;31:1574-1590.e11.
28. Clayton BLL, Barbar L, Sapar M, et al. Patient iPSC models reveal glia-intrinsic phenotypes in multiple sclerosis. *Cell Stem Cell.* 2024;31:1701-1713.e8.

Efficacy made Convenient



TYSABRI SC injection with the potential to administer **AT HOME** for eligible patients*

Efficacy and safety profile comparable between TYSABRI IV and SC^{†1,2}

[†]Comparable PK, PD, efficacy, and safety profile of SC to IV except for injection site pain.^{1,2}

**CLICK HERE TO DISCOVER MORE ABOUT
TYSABRI SC AND THE DIFFERENCE IT MAY
MAKE TO YOUR ELIGIBLE PATIENTS**

Supported by



A Biogen developed and funded JCV antibody index PML risk stratification service, validated and available exclusively for patients on or considering TYSABRI.



*As of April 2024, TYSABRI SC can be administered outside a clinical setting (e.g. at home) by a HCP for patients who have tolerated at least 6 doses of TYSABRI well in a clinical setting. Please refer to section 4.2 of the SmPC.¹

TYSABRI is indicated as single DMT in adults with highly active RRMS for the following patient groups:^{1,2}

- Patients with highly active disease despite a full and adequate course of treatment with at least one DMT
- Patients with rapidly evolving severe RRMS defined by 2 or more disabling relapses in one year, and with 1 or more Gd+ lesions on brain MRI or a significant increase in T2 lesion load as compared to a previous recent MRI

Very common AEs include nasopharyngitis and urinary tract infection. Please refer to the SmPC for further safety information, including the risk of the uncommon but serious AE, PML.^{1,2}

Abbreviations: **AE:** Adverse Event; **DMT:** Disease-Modifying Therapy; **Gd+:** Gadolinium-Enhancing; **HCP:** Healthcare Professional; **IV:** Intravenous; **JCV:** John Cunningham Virus; **MRI:** Magnetic Resonance Imaging; **PD:** Pharmacodynamic; **PK:** Pharmacokinetic; **PML:** Progressive Multifocal Leukoencephalopathy; **RRMS:** Relapsing-Remitting Multiple Sclerosis; **SC:** Subcutaneous.

References: 1. TYSABRI SC (natalizumab) Summary of Product Characteristics. 2. TYSABRI IV (natalizumab) Summary of Product Characteristics.

Adverse events should be reported. For Ireland, reporting forms and information can be found at www.hpra.ie. For the UK, reporting forms and information can be found at <https://yellowcard.mhra.gov.uk/> or via the Yellow Card app available from the Apple App Store or Google Play Store. Adverse events should also be reported to Biogen Idec on MedInfoUKI@biogen.com 1800 812 719 in Ireland and 0800 008 7401 in the UK.